

The influence of charge and flexibility on smectic phase formation in filamentous virus suspensions

Kirstin R. Purdy* and Seth Fraden

*Complex Fluids Group, Martin Fisher School of Physics,
Brandeis University, Waltham, Massachusetts 02454*

(Dated: June 17, 2018)

Abstract

We present experimental measurements of the cholesteric-smectic phase transition of suspensions of charged semiflexible rods as a function of rod flexibility and surface charge. The rod particles consist of the bacteriophage M13 and closely related mutants, which are structurally identical to this virus, but vary either in contour length and therefore ratio of persistence length to contour length, or vary in surface charge. Surface charge is altered in two ways; by changing solution pH and by comparing M13 with *fd* virus, a mutant which differs from M13 only by the substitution of a single charged amino acid for a neutral one per viral coat protein. Phase diagrams are measured as a function of particle length, particle charge and ionic strength. The experimental results are compared with existing theoretical predictions for the phase behavior of flexible rods and charged rods. In contrast to the isotropic-cholesteric transition, where theory and experiment agree at high ionic strength, the nematic-smectic transition exhibits complex charge and ionic strength dependence significantly different from predicted phase behavior. Possible explanations for these unexpected results are discussed.

PACS numbers: 64.70.Md, 61.30.St

*current address: Department of Materials Science and Engineering, University of Illinois at Urbana Champaign, Urbana, Illinois 61801

I. INTRODUCTION

In a suspension of hard or charged rods, purely repulsive entropic interactions are sufficient to induce liquid crystal ordering. Theoretically, hard rods exhibit isotropic, nematic, smectic and columnar liquid crystal phases with increasing concentration [1, 2, 3]. Unfortunately, production of hard, rigid, monodisperse rods is very difficult. Rigid and flexible polyelectrolyte rods, however, are abundant, especially in biological systems, which by nature lend themselves to mass-production. In this paper we will study the influence of flexibility and electrostatic interactions on the formation of a smectic phase from a nematic phase using suspensions of charged, semiflexible *fd* and M13 virus rods. Viruses, such as *fd*, M13, and Tobacco Mosaic Virus are a unique choice for use in studying liquid crystal phase behavior in that they are biologically produced to be monodisperse and are easily modified by genetic engineering and post-expression chemical modification. These virus particles and β -FeOOH rods are, to our knowledge, the only colloidal systems known to exhibit the predicted hard-rod phase progression from isotropic (I) to nematic (N) or cholesteric and then to smectic (S) phases with increasing rod concentration [4, 5, 6]. Even though qualitative theories have been developed to describe either the effects of electrostatics or the effects of flexibility on the nematic-smectic (N-S) phase transition of hard rods [7, 8, 9], they have yet to be thoroughly tested experimentally. Near the N-S transition, the particles are at very high concentrations, and as we will show, dilute-limit approximations of interparticle interactions, which are appropriate at the isotropic-nematic transition, cannot be used. By measuring the N-S transition of charged and/or flexible rods we learn about both the influence of these parameters on smectic phase formation and the interactions between these rods in concentrated suspensions. Additionally, our results add insight into the ordering of other important rodlike polyelectrolytes such as DNA, which often appears in high concentrations under physiological conditions and exhibits cholesteric and columnar, but not the smectic, liquid crystalline phases [10, 11].

In this paper we test the limits of current theoretical predictions for the nematic-smectic phase transition in three ways. First, we measure the phase transition for semiflexible filamentous virus of identical structure and varied length. By changing the rod length and

leaving local particle structure constant, the persistence length P of the rods, defined as one half the Kuhn length, remains constant. Subsequently, the rod flexibility, as defined by the ratio of persistence length to contour length L , or P/L , is altered. In our experiments the flexibility of the particles remains within the semiflexible limit, meaning $P \sim L$. Altering the particle flexibility within the semiflexible limit probes the competition between rigid and flexible rod phase behavior. Second, we vary the ionic strength of the virus rod suspensions allowing us to probe the efficacy of theoretical approximations for incorporating electrostatic repulsion into hard-particle theories. Third, we measure the nematic-smectic phase transition for filamentous virus of different charge. Altering the surface charge by two independent techniques, solution chemistry and surface chemistry, probes the importance of the details of the surface charge distribution in determining long range interparticle interactions. By varying these three independent variables, length, charge and solution ionic strength, we systematically examine how electrostatic interactions and flexibility experimentally effect the nematic-smectic phase boundary.

The colloidal rods we use are the rodlike semiflexible bacteriophages *fd* and M13 which form isotropic (I), cholesteric (nematic) and smectic (S) phases in solution with increasing virus concentration [8, 12, 13, 14]. The free energy difference between the cholesteric and nematic (N) phases is small, and therefore it is appropriate to compare our results with predictions for the nematic phase [15]. Furthermore, near the nematic-smectic transition, the cholesteric unwinds into a nematic phase [16]. M13 and *fd* are composed of 2700 major coat proteins helicoidally wrapped about the single stranded viral DNA. They differ from one another by only one amino acid per major coat protein; the negatively charged aspartate (asp_{12}) in *fd* is substituted for the neutral asparagine (asn_{12}) in M13 [17]. They are thus ideal for use in studying the charge dependence of the virus rod phase transitions. Changes in the surface charge of the particles were also achieved by varying the pH of the solution [18]. Additionally, by varying the length of the M13 DNA we created M13 mutants which differ only in contour length. The M13 mutants have the same local structure, and thus we assume persistence length, as M13. These mutant M13 viruses were used to measure the flexibility dependence of the nematic-smectic phase transition.

II. ELECTROSTATIC INTERACTIONS

For colloidal rods, the total rod-rod interparticle interaction includes a combination of hard core repulsion and long ranged electrostatic repulsion. We present here two ways which have been previously proposed for incorporating electrostatic interactions into hard-rod theories for the nematic-smectic phase transition. The first originates from Onsager's calculation of an effective hard-core diameter (D_{eff}) which is larger than the bare diameter D . D_{eff} is calculated from the second virial coefficient of the free energy for charged rods in the isotropic phase [1]. Specifically, for hard, rigid, rodlike particles, the limit of stability of the isotropic phase against a nematic phase is given by the Onsager relation $bc_i = 4$ where $b = \pi L^2 D/4$ and c_i is the isotropic number density of rods [1]. For charged particles, Onsager showed that the stability condition remains unchanged provided D is replaced with D_{eff} , thus $b_{\text{eff}}c_i = 4$, with $b_{\text{eff}} = \pi L^2 D_{\text{eff}}/4$. Increasing ionic strength decreases D_{eff} , and for highly charged colloids, like M13 and *fd*, D_{eff} is nearly independent of surface charge due to the non-linear nature of the Poisson-Boltzmann equation, which leads to counterion condensation near the colloid surface [13]. In previous work [13, 19], the prediction that $b_{\text{eff}}c_i$ is constant at the I-N phase boundary has been experimentally verified at high ionic strength ($I > 60$ mM, large L/D_{eff}) for our system of virus rods, as illustrated in Fig. 1. These results validated the mapping of the I-N transition of charged virus rods at high ionic strength onto a hard rod theory by using an effective hard diameter, D_{eff} . At low ionic strength ($I < 60$ mM), the prediction that $b_{\text{eff}}c_i$ is constant did not hold because of the breakdown of the second virial approximation at small L/D_{eff} [19]. Consequently, we expect that if D_{eff} works to describe the N-S transition of virus rods it would most likely be at high ionic strengths.

Since D_{eff} is valid only where the second virial approximation is valid, ie. in the isotropic phase, Stroobants *et. al* developed an approximate way to describe the electrostatic interactions in the nematic phase using this second virial approximation [21]. They defined a nematic effective diameter $D_{\text{eff}}^{\text{N}}$, which is calculated from the isotropic effective diameter D_{eff} : $D_{\text{eff}}^{\text{N}} = D_{\text{eff}}[1 + h\eta(f)/\rho(f)]$, where

$$\rho(f) = \frac{4}{\pi} \langle \langle \sin \phi \rangle \rangle \quad (1)$$

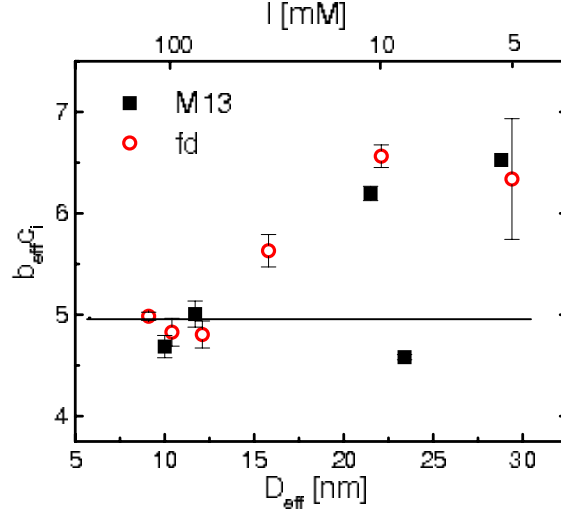


FIG. 1: (Color online) Isotropic-Nematic phase transition $b_{\text{eff}} c_i$ plotted as a function of D_{eff} for both M13 and fd suspensions in Tris-HCl buffer at pH 8.2. The original data for this figure was published previously [19]. The solid line is the hard-rod prediction for semiflexible rods with a persistence length of $2.2 \mu\text{m}$ [20]. For small values of D_{eff} (high ionic strength), the coexistence concentrations for the charged rods are effectively mapped to the hard-rod predictions. The ionic strength scale is for fd suspensions (M13 has a lower surface charge, thus D_{eff} at the same ionic strength is slightly larger).

and

$$\eta(f) = \frac{4}{\pi} \langle \langle -\sin \phi \log(\sin \phi) \rangle \rangle - (\log(2) - 1/2) \rho(f) \quad (2)$$

The average $\langle \dots \rangle$ is over the solid angle Ω weighted by the nematic angular distribution function $f(\Omega)$ with ϕ describing the angle between adjacent rods [22]. The parameter $h = \kappa^{-1}/D_{\text{eff}}$, where κ^{-1} is the Debye screening length, characterizes the preference of charged rods for twisting. Crossed charged rods have a lower energy than parallel charged rods, and h correspondingly increases with increasing electrostatic interactions (decreasing ionic strength). This definition for the nematic effective diameter is accurate as long as the average angle between the rods and the nematic director $\sqrt{\langle \theta^2 \rangle}$ is much greater than $D_{\text{eff}}^{\text{N}}/L$ [23]. In this limit, the second virial coefficient is still much larger than the higher virial coefficients, which can be neglected. Near the N-S transition the order parameter, as determined by x-ray measurements of magnetically aligned samples, is $S = 0.94$ [24]. Using an angular

distribution function with this order parameter of $S = 0.94$ we find that $D_{\text{eff}}^{\text{N}} = 1.16D_{\text{eff}}$ at 5mM ionic strength and $D_{\text{eff}}^{\text{N}} = 1.10D_{\text{eff}}$ at 150 mM ionic strength. This corresponds to $\sqrt{\langle\theta^2\rangle} \sim 6D_{\text{eff}}^{\text{N}}/L$ for the largest value of $D_{\text{eff}}^{\text{N}}$.

Previously, we argued that $D_{\text{eff}}^{\text{N}}$, which is independent of virus concentration, could describe the electrostatic interactions of *fd* virus suspensions at the nematic-smectic transition [8]. However, as mentioned above, the use of D_{eff} beyond the regime where the second virial coefficient quantitatively describes the system is not justified, and from our calculation of $\sqrt{\langle\theta^2\rangle}$ we know the use of the second virial approximation is questionable. In this article, our expanded range of measurements of the N-S transition of virus suspensions as a function of ionic strength, virus length, and virus surface charge will demonstrate that electrostatic interactions at the nematic-smectic transition are much more complex than those predicted at the limit of the second virial coefficient.

An alternative method for incorporating electrostatics into a hard-rod theory for the N-S transition was developed by Kramer and Herzfeld. They calculate an “avoidance diameter” D_{a} which minimizes the scaled particle expression for the free energy of charged parallel spherocylinders as a function of concentration [7]. With respect to ionic strength, D_{a} exhibits the same trend as D_{eff} , but unlike D_{eff} , D_{a} is inherently concentration dependent, decreasing with increasing rod concentration. D_{a} can never be greater than the actual rod separation, something which is not impossible with D_{eff} . Furthermore, by using the scaled particle theory, third and higher virial coefficients are accounted for in an approximate way [25, 26], unlike Onsager’s effective diameter. This makes the “avoidance diameter” more appropriate for incorporating electrostatic interactions at the nematic-smectic transition. One disadvantage with the free energy expression developed by Kramer and Herzfeld is that it does not reduce to Onsager’s theory in the absence of electrostatic interactions. Nevertheless, Kramer and Herzfeld’s calculations do qualitatively reproduce previously published data for the N-S transition of *fd* virus [7]. However, the limited range of data previously available did not include some of the interesting features described in this theory, which we are now able to test.

III. MATERIALS AND METHODS

Properties of the wild type (*wt*) virus *fd* and M13 include their length $L = 0.88 \mu\text{m}$, diameter $D = 6.6 \text{ nm}$, and persistence length $P = 2.2 \mu\text{m}$ [5]. The M13 mutants have the same diameter as the wild type M13 and lengths of $1.2 \mu\text{m}$, $0.64 \mu\text{m}$, and $0.39 \mu\text{m}$ [14]. Because the molecular weight of the virus is proportional to its length, the molecular weight of the M13 mutants is $M = M_{wt}L/L_{wt}$, with $M_{wt} = 1.64 \times 10^7 \text{ g/mol}$ and $L_{wt} = 0.88 \mu\text{m}$, the molecular weight and length of wild type M13, respectively. Virus production is explained elsewhere [27]. Two of the length-mutants ($0.64 \mu\text{m}$ and $0.39 \mu\text{m}$) were grown using the phagemid method [14, 27], which produces bidisperse solutions of the phagemid and the $1.2 \mu\text{m}$ helper phage. Sample polydispersity was checked using agarose gel electrophoresis on the intact virus, and on the viral DNA. Excepting the phagemid solutions which were 20% by mass $1.2 \mu\text{m}$ helper phage, virus solutions were highly monodisperse as indicated by sharp electrophoresis bands. All of these virus suspensions form well defined smectic phases [14].

All samples were dialyzed against a 20 mM Tris-HCl buffer at pH 8.2 or 20 mM Sodium Acetate buffer adjusted with Acetic Acid to pH 5.2. To vary ionic strength, NaCl was added to the buffering solution. The linear surface charge density of *fd* is approximately $10 \text{ e}^-/\text{nm}$ ($3.4 \pm 0.1 \text{ e}^-/\text{coat protein}$) at pH 8.2 and $7 \text{ e}^-/\text{nm}$ ($2.3 \pm 0.1 \text{ e}^-/\text{coat protein}$) at pH 5.2 [18]. The M13 surface charge is $7 \text{ e}^-/\text{nm}$ ($2.4 \pm 0.1 \text{ e}^-/\text{coat protein}$) at pH 8.2 and $3.6 \text{ e}^-/\text{nm}$ ($1.3 \pm 0.1 \text{ e}^-/\text{coat protein}$) as determined by comparing the M13 composition and electrophoretic mobilities to those of *fd* [19]. On the viral surface, *fd* has four negatively ionizable amino acids and one positively ionizable amino acid per coat protein. At neutral pH, the terminal amine contributes approximately $+1/2 \text{ e}$ charge. The M13 surface has three negatively ionizable amino acids, one positively ionizable amino acid and the terminal amine ($+1/2 \text{ e}$) per coat protein.

After dialysis, the virus suspensions were concentrated via ultracentrifugation at 200 000g and diluted to concentrations just above the N-S transition. Virus suspensions were then allowed to equilibrate to room temperature. Bulk separation of the nematic and smectic phases is not observed, perhaps because of the high viscosity of the suspensions near the

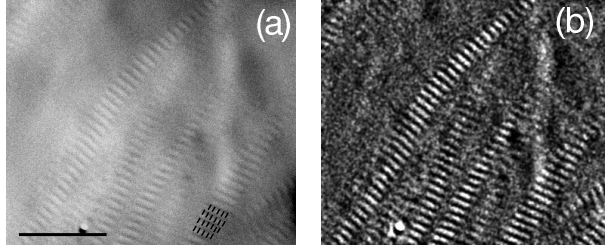


FIG. 2: (a) Differential interference contrast microscopy image of nematic-smectic coexistence of *fd* virus suspensions. The smectic phase can be recognized by the ladder like structures. The virus rods are oriented perpendicular to the layers as illustrated. The uniform texture is the nematic phase. (b) Digitally enhanced image of (a). The scale bar is 10 μm .

N-S transition. However, smectic or nematic domains can be observed using differential interference contrast microscopy in coexistence with predominantly nematic and smectic bulk phases, respectively. Typically coexistence is observed as ribbons of smectic phase reaching into a nematic region, as shown in Fig. 2.

The location of the N-S transition was determined by measuring the highest nematic volume fraction (ϕ^N) and the lowest smectic volume fraction (ϕ^S) observed. The volume fraction $\phi^S = c^S v$, where c^S is the number density, and v is the volume of a single rod $\pi L D^2/4$. A similar equation holds for ϕ^N . The concentration of the phases was measured by absorption spectroscopy with the optical density (A) of the virus being $A_{269\text{nm}}^{1\text{mg/ml}} = 3.84$ for a path length of 1 cm.

Since knowing the surface charge of the virus is critical to our analysis of the N-S transition, we experimentally measured the pH of the virus solutions at concentrations in the nematic phase just below the N-S transition. We found that for an initial buffer solution at pH 8.2 (Tris-HCl buffer $\text{pKa} = 8.2$), the pH of the concentrated virus suspensions is slightly less than 8.2, but still well within the buffering pH range ($\text{pH} = \text{pKa} \pm 1$). The surface charge does not change significantly over this range [18]. At pH 5.2 (Acetic acid buffer $\text{pKa} = 4.76$) the measured pH of the virus suspensions near the N-S transition was slightly higher than 5.2, with pH increasing slightly with decreasing ionic strength, most likely due to the relatively high concentration of virus counterions (50-100 mM) as compared to buffer ions (20 mM). This shift further away from the pKa may influence the phase behavior by increasing

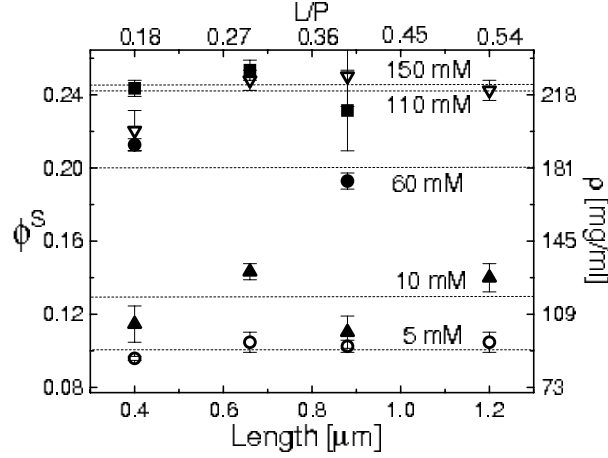


FIG. 3: Volume fraction at the nematic-smectic phase transition, ϕ^S , for multiple ionic strengths at pH 8.2 as a function of rod length L and flexibility L/P . On the right axis is the measured concentration in mass density $\rho^S = \phi^S M / v N_a$, where N_a is Avagadro's number. Legend for ionic strengths is as follows: \circ 5 mM, \blacktriangle 10 mM, \bullet 60 mM, ∇ 110 mM, \blacksquare 150 mM. With increasing ionic strength ϕ^S increases due to increasing electrostatic screening. Dashed lines are a guide to the eye at constant ionic strength. Within experimental accuracy the smectic phase transition is independent of flexibility within the range $0.18 < L/P < 0.54$.

the the viral surface charge. The implications of these measurements are discussed in the Results section.

IV. RESULTS

A. Flexibility and ionic strength dependence of the N-S transition

Fig. 3 shows ϕ^S as a function of the M13 mutant particle length, and therefore virus flexibility by L/P , for multiple ionic strengths. Focusing on how rod flexibility influences the phase transition, we observe that at each ionic strength the measured ϕ^S is independent of virus length, within experimental accuracy, and thus independent of changing flexibility in the range of $0.18 < L/P < 0.54$. The bidispersity of the $0.64 \mu\text{m}$ and $0.39 \mu\text{m}$ rod suspensions does not seem to influence the phase boundary because these samples, which are 20% $1.2 \mu\text{m}$ rods by mass exhibit the same phase behavior as samples which are 100% $1.2 \mu\text{m}$ rods.

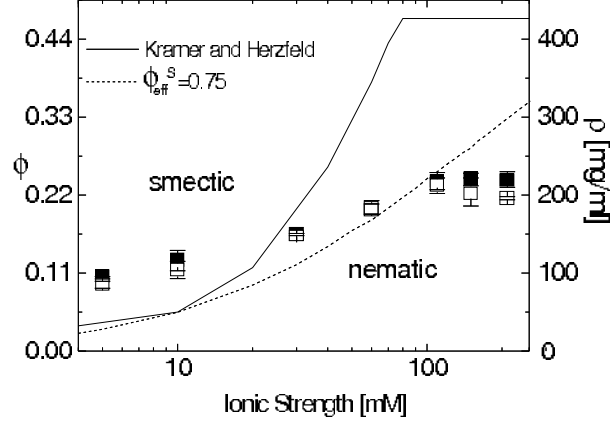


FIG. 4: Average values of ϕ^N (open) and ϕ^S (solid) at the N-S transition as a function of ionic strength at pH 8.2. Average at each ionic strength is over the results for the four M13 length mutants. The solid line is ϕ^S taken from simulations by Kramer and Herzfeld [7] for the N-S transition of particles the same size as *fd* and with a renormalized surface charge of $1e^-/7.1 \text{ \AA}$. The dashed line is $\phi^S = \phi_{\text{eff}}^S * D^2 / (D_{\text{eff}}^N)^2$ with $\phi_{\text{eff}}^S = 0.75$.

As the N-S phase transition is independent of rod flexibility for these experiments, we averaged the results for ϕ^S and ϕ^N from all particle lengths to study the ionic strength dependence of the phase transition. These averaged values for ϕ^S and ϕ^N are shown as a function of ionic strength in Fig. 4. We observe that with increasing ionic strength, and therefore a corresponding decrease in electrostatic interactions, the volume fraction of the phase transition increases until an ionic strength of approximately $I = 100 \text{ mM}$, at which point the phase transition becomes independent of ionic strength. Whereas the increase in phase transition concentration with ionic strength has been observed previously for suspensions of *fd* virus [8], the plateau in ϕ^S and ϕ^N at high ionic strengths is previously undocumented.

B. Surface charge dependence of the N-S transition

To determine the influence of virus surface charge on N-S phase transition, we measured phase behavior of *fd* and M13 at both pH 8.2 and pH 5.2. Fig. 5 presents the ionic strength and pH dependence of the N-S phase transition for *fd* (a) and M13 (b). Below 100 mM, there is a strong pH dependence in the N-S transition, as shown in Fig. 5a,b.

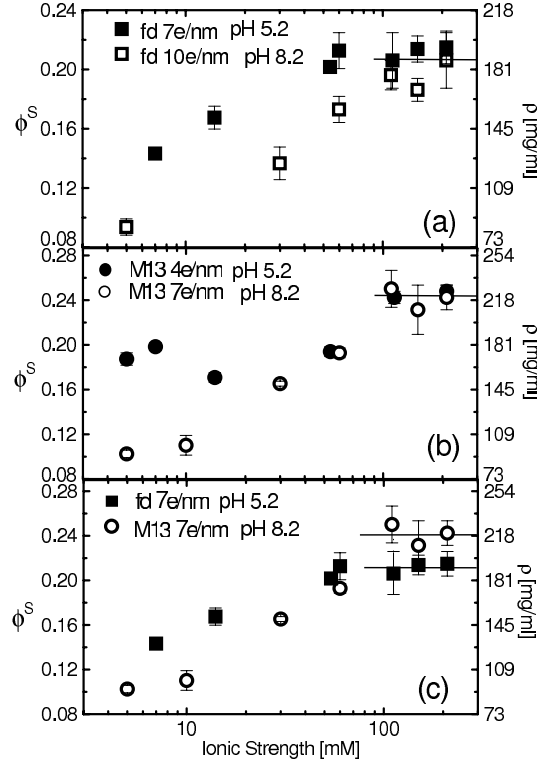


FIG. 5: Nematic-smectic phase transition volume fraction ϕ^S as function of ionic strength for suspensions of a) *fd* and b) M13 at pH 5.2 (solid) and pH 8.2 (open). Figure c) shows M13 (pH 8.2) and *fd* (pH 5.2) at 7 e/nm surface charge. Solid lines highlight the ionic strength independence at high ionic strength.

Suspensions at higher pH (higher surface charge) consistently enter a smectic phase at lower concentrations. Above about 100 mM, ϕ^S is independent of ionic strength, as in Fig. 4. The *fd* phase boundary at high ionic strength saturates around $\phi_{\text{sat}}^S \sim 0.21$, independent of pH, and the M13 phase boundary saturates around $\phi_{\text{sat}}^S = 0.24$, also independent of pH. Even at these high ionic strengths, where the surface charge of the virus is well screened, the higher charged *fd* suspensions have a phase boundary at lower concentrations than the M13 suspensions.

In Fig. 5c we compare the phase transition for M13 and *fd* suspensions when both viruses have the same surface charge of $7e^-/\text{nm}$. Because the rods have the same surface charge, we assume the rods differ only by the location of the charges (positive and negative) on the surface. At low ionic strength the phase behavior is similar, but *fd* suspensions consistently

enter the smectic phase at a slightly higher concentration. We note that the small measured increase in pH at low ionic strength of the pH 5.2 viral solutions mentioned in the Materials and Methods section does not account for this difference. An increase in pH would lower, not raise, the pH 5.2 phase transition concentrations by increasing electrostatic interactions. At high ionic strength, the reverse is true; *fd* has a lower phase transition concentration than M13 suspensions, as mentioned above. We believe the measured differences in ϕ_{sat}^S between M13 and *fd* to be statistically significant, and will discuss this unexpected observation further in the following section.

V. DISCUSSION

A. Flexibility and ionic strength dependence of the N-S transition

The nematic-smectic transition of flexible, hard rods has been studied both theoretically and computationally [3, 9, 28]. A small amount of flexibility is expected to drive the smectic phase to higher concentrations, from the predicted hard-rigid-rod concentration of $\phi^S=0.47$ [2], to approximately $0.75 \lesssim \phi^S \lesssim 0.8$ within the semiflexible limit [9]. Within the semiflexible limit ($L/P \sim 1$), however, ϕ^S is predicted to be essentially independent of flexibility [9]. This insensitivity of ϕ^S to flexibility in the semiflexible limit is in agreement with the measurements presented in Fig. 3. We note that this result is in striking contrast to the significant flexibility dependence measured at isotropic-nematic transition for this same system of semiflexible M13 mutants which we describe in a separate report [19].

As our rods are charged, the ionic strength of the virus suspension plays an important role in determining the phase boundaries by screening electrostatic interactions. To compare our charged-flexible-rod results with current predictions for the N-S phase transition of hard (rigid or flexible) rods, we have to effectively account for the electrostatic interactions between our virus rods. Two methods for incorporating electrostatics into the N-S phase transition of hard rods [7, 22, 23] were presented earlier in this paper. One way to do this is to graph ϕ_{eff}^S , the measured effective volume fraction along the nematic-smectic transition, and compare it to the theoretical volume fraction, ϕ_{th}^S , for the N-S transition of hard, semiflexible

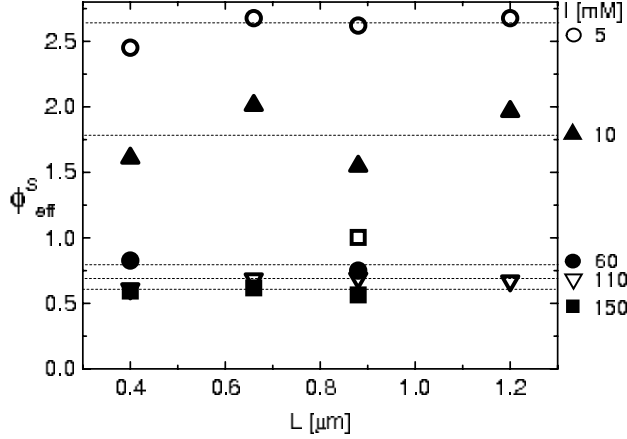


FIG. 6: Effective volume fraction volume fraction along the nematic-smectic phase transition $\phi_{\text{eff}}^S = \phi^S(D_{\text{eff}}^N)^2/D^2$ for multiple ionic strengths at pH 8.2 as a function of L . ϕ^S , the actual volume fraction at the N-S transition, is shown in Fig. 3. Legend for symbols is to the right of the figure. Dashed lines drawn are a guide to the eye and are at constant ionic strength. Because ϕ_{eff}^S strongly depends on ionic strength, we conclude that D_{eff}^N does not describe the electrostatic interactions at high virus concentrations.

rods [3, 9]. ϕ_{eff}^S is defined as $c^S \pi L (D_{\text{eff}}^N)^2 / 4 = \phi^S (D_{\text{eff}}^N)^2 / D^2$ and is shown in Fig 6. If the effect of electrostatics can be accounted for by replacing D with D_{eff}^N , as can be done at the isotropic-nematic transition at high ionic strength, we could predict that $\phi_{\text{eff}}^S = \phi_{\text{th}}^S = 0.75$. In other words, if D_{eff}^N accurately models the interparticle electrostatic interactions, the effective volume fraction ϕ_{eff}^S should be equivalent to the hard-flexible rod volume fraction and should be independent of ionic strength. Thus multiplying the measured values for ϕ^S shown in Fig. 3 by $(D_{\text{eff}}^N)^2/D^2$ should result in the collapse of all the different ionic strength data.

However, we find that ϕ_{eff}^S depends quite strongly on ionic strength in Fig. 6. Previously, we observed $\phi_{\text{eff}}^S = 0.75$ independent of ionic strength for suspensions of *fd* virus [8]. The data in Fig. 6 is consistent with this value at high ionic strengths ($60\text{mM} < I < 150\text{ mM}$), but by including a larger range of ionic strengths as well as multiple particle lengths, we clearly observe an ionic strength dependence in ϕ_{eff}^S , with ϕ_{eff}^S ranging from 2.5 to 0.5. Furthermore, the plateau in the phase transition concentration at high ionic strength is not captured by scaling ϕ^S by $(D_{\text{eff}}^N)^2/D^2$, as shown in Fig. 4 by the dashed curve for $\phi_{\text{eff}}^S = 0.75$. The large ionic strength dependence of ϕ_{eff}^S , and the measured ionic strength independence above

100 mM indicate that $D_{\text{eff}}^{\text{N}}$ is inadequate for describing the electrostatic interactions at the N-S transition. This is in contrast to the I-N transition, where D_{eff} accurately incorporates the electrostatic interactions between virus rods at high ionic strength [19]. Furthermore, because $\phi_{\text{eff}}^{\text{S}} > 1$ at low ionic strength we conclude that $D_{\text{eff}}^{\text{N}}$ overestimates the electrostatic interactions. This is not surprising because $D_{\text{eff}}^{\text{N}}$ is based on the second virial approximation which, strictly speaking, is valid only for isotropic suspensions at low concentrations. Using D_{eff} to relate the phase behavior of charged rods to hard-rod predictions is inappropriate at the N-S transition, particularly at high ionic strengths.

The plateau in ϕ^{S} at high ionic strength is indeed predicted for parallel, charged, rigid spherocylinders with a concentration dependent avoidance diameter D_{a} , as shown by the solid line in Fig 4. This avoidance model predicts that at high ionic strength ϕ^{S} saturates at $\phi_{\text{sat}}^{\text{S}} = 0.47$, the theoretical value for hard, rigid spherocylinders [2, 7]. Because our rods are semiflexible, we would correspondingly predict that $\phi_{\text{sat}}^{\text{S}}$ would be equal to the theoretical value for hard-semiflexible rods, $\phi_{\text{th}}^{\text{S}} = 0.75$. Instead of this value, our measurements of the phase transition volume fraction as a function of ionic strength yield $\phi_{\text{sat}}^{\text{S}} = 0.21 - 0.24$, which is three times lower than predicted by hard flexible rod theories. This suggests that either the flexibility of the rods has lowered the phase transition from that of hard rods, in contradiction to both theories and simulations, or that the electrostatic interactions between the rods are not accurately represented by either D_{a} or D_{eff} . We will return to this question at the end of the Discussion section.

B. Surface charge dependence of the N-S transition

The pH dependence of the phase transition visible in Fig. 5, and the difference between M13 and *fd* saturation concentrations present even when they share the same surface charge (Fig. 5c) also indicate that neither D_{eff} nor D_{a} are appropriate for describing the electrostatic interactions between the virus rods at the N-S transition. The non-linearity of the Poisson-Boltzmann equation predicts that for high linear charge density the long-range electrostatic potential between rods is insensitive to surface charge changes and thus pH changes [1, 21]. This is confirmed at the isotropic-nematic transition, where the charge dependence is well

described by D_{eff} and the pH dependence of the phase transition is very small [19]. However, a strong pH dependence of the smectic phase transition at low ionic strengths for both *fd* (Fig. 5a) and M13 (Fig. 5b) suspensions is observed. The observed difference between M13 and *fd* saturation concentrations at high ionic strength and equal surface charge (Fig. 5c) is also not expected from Poisson-Boltzmann theory. This high sensitivity of the N-S transition to changes in pH and surface charge configuration indicates that the charge independent nature predicted by both D_{eff} and D_a does not correctly characterize the electrostatic interactions at the concentrations of the N-S transition.

One possible explanation for why the high ionic strength, and correspondingly high concentration, phase behavior is sensitive to surface charge configuration is that the adjacent virus surfaces are separated by approximately one virus diameter (6.6 nm) [24], which is on the order of the spacing between viral coat-proteins (1.6 nm), and the Debye screening length $\kappa = 3.0\text{\AA}/\sqrt{I} = 9\text{\AA}$. When the surface to surface distance is of the order of the Debye screening length, the continuous charge distribution approximation used in Poisson Boltzmann theory can no longer be used, as is done in the effective diameter calculations. Furthermore, it has been shown theoretically that discretization of the surface charges can change the predicted counterion condensation from that predicted by the non-linear Poisson Boltzmann equation [29, 30]. Perhaps it is because we are in the regime where the surface charge configuration can no longer be neglected that we observe charge-configuration-dependent saturation of the nematic-smectic phase transition. Previous work by Lyubartsev *et. al.* has been done to simulate the electrostatic interactions between these virus rods in the presence of divalent ions using an approximate discrete charge configuration [31]. We propose that theoretical models or simulations similar to those by Lyubartsev *et. al* of the electrostatic interactions of a dense, rod-like polyelectrolyte system which include the detail of the surface charge configuration including the location of positive and negative amino acids on the viral surface, may shed light on the experimental differences between M13 and *fd* nematic-smectic transitions at high ionic strength.

C. Origin of the ionic strength independence of the NS transition

At high ionic strength we have measured an ionic strength independent N-S transition. This is similar to the phase behavior predicted by Kramer and Herzfeld, in which the phase transition volume fraction saturates at that predicted for the N-S transition of hard rods. Yet, the value for our measured ϕ_{sat}^S is three times lower than the predicted N-S transition volume fraction for semi-flexible rods $\phi_{\text{th}}^S = 0.75$. These observations point to a failure of theory to describe the role of electrostatics and/or flexibility on the N-S transition.

It has been shown by Odijk that undulations of semiflexible rods in a hexagonal configuration are typically contained within a tube of a diameter larger than the bare rod diameter [32]. These undulations create an effective repulsion similar to Helfrich repulsion of membranes. The dominant interaction between charged flexible rods in a dense suspension therefore depends on the relative size of the tube diameter and the electrostatic effective diameter [33]. At low ionic strength the interparticle interactions would be dominated by electrostatics, and at high ionic strength the interparticle interactions would be dominated by steric interactions of the flexible rods. This simple argument qualitatively agrees with our observed phase behavior. If charged, flexible rod behavior is indeed dominated by steric interactions at high ionic strengths, we expect that the N-S phase transition would be at a value equal to that predicted by theory for hard-semiflexible rods. However, both theory and simulations for hard-flexible rods which incorporate this repulsion due to flexibility, predict that flexibility destabilizes the N-S transition, subsequently increasing, not decreasing as measured, the transition concentration above that predicted for rigid rods [3, 9, 34]. It is possible that the role of flexibility is not accurately incorporated into the theories which predict an increase in ϕ^S from that predicted for rigid rods. However, we believe these theories to be accurate, specifically because simulations by Polson and Frenkel of hard semiflexible rods demonstrate that flexibility increases the N-S transition concentration above that predicted for rigid rods [3].

A second possible explanation for the discrepancy between our experimental values of ϕ_{sat}^S and the predicted values for the phase transition of semiflexible hard rods is that the electrostatic interactions between the rods are indeed significant at high ionic strength, and that

they are different from the predicted electrostatic interactions. As our measurements suggest that both the second virial and avoidance approximations for the electrostatic interactions describe a N-S transition which differs significantly from the experimentally observed behavior, we believe this is possible. Further evidence to suggest that electrostatics still plays a role at high ionic strength is visible in Fig. 5 which shows that the surface charge of the rods can still influence the phase behavior, even when the phase transition has become ionic strength independent.

A third possibility is that coupling electrostatics and flexibility produces an inter-rod repulsion which is a complex combination of flexible-hard rod and charged-rigid rod interactions. It has been shown for concentrated suspensions of DNA, that fluctuations due to the flexibility of the DNA actually enhance inter-rod repulsions in an exponential manner [35]. The consequence is that for a given osmotic pressure exerted by a concentrated DNA suspension, the volume fraction of DNA is much lower than predicted by Poisson-Boltzmann electrostatics alone. This hypothesis is consistent with our measurements of a ϕ_{sat}^S that is much lower than predicted for both rigid and flexible rods.

As our results are quite unexpected with respect to current theoretical predictions for the nematic - smectic transition of rod suspensions, we have speculated as to possible explanations for our observations. To fully understand the phase behavior of charged, flexible rods further computational and theoretical work is clearly needed.

VI. CONCLUSION

We have examined the nematic-smectic phase diagram for charged, semiflexible virus rods as a function of length, surface charge and ionic strength. We observed that in the semiflexible-rod limit the N-S phase boundary is independent of rod flexibility, as predicted theoretically. However, by studying the ionic strength dependence of this transition we observed that renormalizing the measured phase transition volume fraction, ϕ^S , by Onsager's effective diameter, D_{eff} , does not produce an ionic-strength independent phase transition concentration. Therefore the second virial approximation cannot be used to map the measured nematic - smectic phase transition of charged, flexible rods onto hard, flexible rod

theories.

At high ionic strength, we found that the concentration of the N-S phase boundary is independent of ionic strength. Kramer and Herzfeld's avoidance diameter theory [7] qualitatively reproduces the observed ionic strength independent N-S phase behavior, but predicts that the ionic strength independent phase boundary is equal to the predicted hard-rod phase boundary. Our experimental results, however, are three times lower than the hard-particle phase boundary predicted for semiflexible rods, ϕ_{th}^S [3, 9]. Clearly, more theoretical work is needed to understand the nematic-smectic phase transition of charged, flexible rods, in order to reconcile the differences we observe with charged, flexible viruses and that reported in simulations of hard, flexible rods.

Finally, significant differences were measured between M13 and *fd* nematic-smectic phase transition concentrations, even when they shared the same average surface charge. These results indicate that the electrostatic interactions between these rods are more complicated than can be accounted for by calculating the interparticle potential assuming a uniform renormalized surface charge. We hypothesize that the electrostatic interactions between rods is influenced by the configuration of the charged amino acids on the viral surface. Experimental tests of this hypothesis could be made by measuring M13 and *fd* equations of state (pressure vs density), and thus the particle-particle interactions, as a function of solution salt and pH, as in techniques developed for DNA [35]. Computationally, this hypothesis can be tested by calculating the pair potential between rods with discrete charges [31].

Acknowledgments

We acknowledge support from the NSF(DMR-0088008).

-
- [1] L. Onsager, Ann. NY Acad. Sci. **51**, 627 (1949).
 - [2] P. G. Bolhuis and D. Frenkel, J. Chem. Phys. **106**, 668 (1997).
 - [3] J. M. Polson and D. Frenkel, Phys. Rev. E **56**, R6260 (1997).

- [4] R. B. Meyer, in *Dynamics and Patterns in Complex Fluids*, edited by A. Onuki and K. Kawasaki (Springer-Verlag, 1990), p. 62.
- [5] S. Fraden, in *Observation, Prediction, and Simulation of Phase Transitions in Complex Fluids*, edited by M. Baus, L. F. Rull, and J. P. Ryckaert (Kluwer Academic, Dordrecht, 1995), pp. 113–164.
- [6] H. Maeda and Y. Maeda, Phys. Rev. Lett. **90**, 018303 (2003).
- [7] E. M. Kramer and J. Herzfeld, Phys. Rev. E **61**, 6872 (2000).
- [8] Z. Dogic and S. Fraden, Phys. Rev. Lett. **78**, 2417 (1997).
- [9] A. V. Tkachenko, Phys. Rev. Lett. **77**, 4218 (1996).
- [10] R. Podgornik, H. Strey, and V. Parsegian, Curr. Op. in Colloid and Interface Science **3**, 534 (1998).
- [11] F. Livolant, A. Levelut, J. Doucet, and J. Benoit, Nature **339**, 724 (1989).
- [12] J. Lapointe and D. A. Marvin, Mol. Cryst. Liq. Cryst. **19**, 269 (1973).
- [13] J. Tang and S. Fraden, Liquid Crystals **19**, 459 (1995).
- [14] Z. Dogic and S. Fraden, Phil. Trans. R. Soc. Lond. A. **359**, 997 (2001).
- [15] P. G. de Gennes and J. Prost, *The Physics of Liquid Crystals* (Oxford Science, 1993), 2nd ed.
- [16] Z. Dogic and S. Fraden, Langmuir **16**, 7820 (2000).
- [17] D. A. Marvin, R. D. Hale, C. Nave, and M. H. Citterich, J. Molec. Bio. **235**, 260 (1994).
- [18] K. Zimmermann, J. Hagedorn, C. C. Heuck, M. Hinrichsen, and J. Ludwig, J. Biol. Chem. **261**, 1653 (1986).
- [19] K. R. Purdy and S. Fraden, Phys. Rev. E **70**, 061703 (2004).
- [20] Z. Y. Chen, Macromolecules **26**, 3419 (1993).
- [21] A. Stroobants, H. N. W. Lekkerkerker, and D. Frenkel, Phys. Rev. Lett. **57**, 1452 (1986).
- [22] A. Stroobants, H. N. W. Lekkerkerker, and T. Odijk, Macromolecules **19**, 2232 (1986).
- [23] G. J. Vroege and H. N. W. Lekkerkerker, Rep. Prog. Phys. **55**, 1241 (1992).
- [24] K. R. Purdy, Z. Dogic, S. Fraden, A. Rühm, L. Lurio, and S. G. J. Mochrie, Phys. Rev. E **67**, 031708 (2003).
- [25] M. A. Cotter and D. C. Wacker, Phys. Rev. A **18**, 2669 (1978).

- [26] M. A. Cotter, in *The Molecular Physics of Liquid Crystals*, edited by G. R. Luckhurst and G. W. Gray (Academic Press, London, 1979), pp. 169–189.
- [27] J. Sambrook, E. F. Fritsch, and T. Maniatis, *Molecular Cloning: A Laboratory Manual* (Cold Spring Harbor Laboratory, New York, 1989), 2nd ed.
- [28] P. van der Schoot, J. Phys. II France **6**, 1557 (1996).
- [29] C. J. Marzec and L. A. Day, Biophys. J. **67**, 205 (1994).
- [30] M. L. Henle, C. D. Santangelo, D. M. Patel, and P. A. Pincus, Europhys. Lett. **66**, 284 (2004).
- [31] A. P. Lyubartsev, J. X. Tang, P. A. Janmey, and L. Nordenskiöld, Phys. Rev. Lett. **81**, 5465 (1998).
- [32] T. Odijk, Macromolecules **19**, 2313 (1986).
- [33] T. Odijk, Biophys. Chem. **46**, 69 (1993).
- [34] R. C. Hidalgo, D. E. Sullivan, and J. Z. Y. Chen, Phys. Rev. E **71**, 041804 (2005).
- [35] H. H. Strey, V. A. Parsegian, and R. Podgornik, Phys. Rev. Lett. **78**, 895 (1997).